JURNAL UPI

Indonesian Journal of Science & Technology

Journal homepage: http://ejournal.upi.edu/index.php/ijost/

IJoST Indonesian Journal of Science & Technology

Integrating Ground Magnetic and Satellite Gravity Data for Delineating Geothermal System-Controlling Structures

Justinus Satrio[1,2], Arga Nanda Aprilla[2], Sukir Maryanto[2], Mayang Bunga Puspita[2], Iskara Hadijah Aqila Nasywa Rastramata Athorhab[2], Rifqi Rizmanda Abidin[2], Elizza Inaya Permata Sari[2], Sri Dwi Wuryani[3], Herman Tolle[2], Emad M.H. Takla[4,5]*

[1]L'ile Croix International Hospitality, Colorado, USA
[2]Brawijaya University, Malang, Indonesia
[3]Indonesian Agency for Meteorology, Climatology, and Geophysics, Jakarta, Indonesia
[4]Kyushu University, Fukuoka, Japan
[5]National Research Institute of Astronomy and Geophysics (NRIAG), Helwan, Egypt
*Correspondence: E-mail: sukir@ub.ac.id

ABSTRACT

Geothermal energy is a key renewable resource in Indonesia, including non-volcanic regions where subsurface conditions remain poorly understood. The Karangrejo–Tinatar area in Pacitan, East Java, displays hot spring manifestations that suggest a structurally controlled geothermal system. This study characterises the system using integrated primary ground magnetic data and GGMPlus satellite gravity data over a 25 km² area. Magnetic data were processed using Reduction to the Pole and Tilt Derivative, while gravity data were analysed through Bouguer correction, upward continuation, and 3D inversion modelling with ZondGM3D and Grablox 1.6. Results show magnetic susceptibility values ranging from −0.01759 to 0.0402 SI and rock density values from 1.88 to 3.11 g/cm³. The inversion model identified five major fault structures—Kebonsari, X, Karangrejo, Sedayu, and Tinatar Faults—that control geothermal fluid circulation as recharge and discharge pathways. This study provides a new framework for understanding non-volcanic geothermal systems in Indonesia.

ARTICLE INFO

Article History:
Submitted/Received 10 Dec 2025
First Revised 11 Mar 2026
Accepted 07 Apr 2026
First Available Online 29 Apr 2026
Publication Date 30 Apr 2026

Keyword:
Geological structure,
Geothermal system,
Gravity,
Karangrejo-Tinatar,
Magnetic.

1. INTRODUCTION

Indonesia has shown a strong commitment to developing renewable energy. Geothermal energy stands out among various renewable energy sources due to its significant potential in Indonesia. In addition to reducing reliance on fossil fuels, geothermal energy supports global climate change mitigation efforts by lowering greenhouse gas emissions from the combustion of fossil fuels [1-2]. The National Energy General Plan (RUEN) outlined the plan targets increasing the contribution of renewable energy to 23% of the total national energy mix by 2025 and 31% by 2050.

Indonesia's tectonic location along the Pacific "Ring of Fire" positions the country as one of the global leaders in geothermal potential, encompassing volcanic and non-volcanic systems [3-4]. East Java, the primary focus of this research region, has a complex tectonic structure which controlled by several active faults [5]. These active faults play an important role in the geothermal system by providing natural pathways through permeable rock zones [6], furthermore, this geothermal system is also referred to as a fault-hosted geothermal system [7]. One of the notable areas for non-volcanic geothermal potential is the Karangrejo-Tinatar region in Pacitan Regency, East Java [8]. Surface manifestations such as hot springs indicate the presence of a subsurface geothermal system.

Theoretically, geothermal energy results from heat convection from the Earth's interior [9] which driven by natural radioactive isotopes such as thorium, uranium, and potassium [10], stored within a reservoir [11]. These reservoirs are controlled by geological structures that act as traps for hot fluids. Faults and fractures facilitate fluid migration to the surface, resulting in geothermal manifestations such as hot springs [12]. Therefore, geological structure analysis using gravity and magnetic data is essential to understanding the geological controls of geothermal systems, especially in non-volcanic areas like Karangrejo-Tinatar [13]. Geophysical methods based on gravity and magnetic data provide effective tools for characterizing subsurface conditions through variations in rock density and magnetic susceptibility. These methods are particularly useful for identifying geological structures such as faults and fracture zones that control geothermal fluid circulation. In addition, three-dimensional inversion modeling enables improved interpretation of subsurface structural continuity and geothermal fluid migration pathways, thereby supporting more reliable geothermal system characterization.

Exploration of non-volcanic geothermal systems, often referred to as fault-hosted geothermal systems, has gained increasing attention due to their potential as a clean energy source outside active magmatic environments [14-15]. These systems are typically controlled by shallow fault structures that allow hot fluids to circulate to the surface [15]. In recent years, both gravity and magnetic methods have proven effective for identifying subsurface structures and reservoir systems in non-volcanic geothermal areas [14, 16]. The integration of these two datasets enables more robust subsurface modelling by simultaneously constraining density and magnetic susceptibility distributions [17].

Previous geothermal investigations have predominantly focused on volcanic systems or relied on single geophysical datasets [18-19], limiting structural characterisation of tectonically controlled prospects. The Karangrejo-Tinatar area remains poorly understood, particularly regarding its fluid pathways and structural controls. Although Puspita *et al.* [18] identified NW-SE trending faults controlling hot springs using ground-gravity, and Widiyansari *et al.* [19] characterised reservoir rocks from satellite gravity data, no study has conducted primary ground magnetic surveys covering both manifestation zones. Sumotarto *et al.* [20] provided regional geological context by documenting the Mandalika and Arjosari Formations.

DOI: https://doi.org/10.17509/ijost.v11i1.93666
p- ISSN 2528-1410 e- ISSN 2527-8045

However, no study to date has conducted primary ground magnetic surveys covering both geothermal manifestation zones, and multi-scale integration of magnetic, gravity, and geological data has not been systematically applied. This limits the ability to characterise the full structural framework controlling fluid pathways in the Karangrejo–Tinatar area.

This study aims to develop an integrated 3D subsurface model of the Karangrejo–Tinatar geothermal prospect through ground magnetic measurements, satellite gravity data, and geological observations, with specific objectives to identify major fault structures controlling geothermal manifestations, analyze the relationship between rock density and magnetic susceptibility distributions, and delineate potential geothermal fluid migration pathways. By presenting a high-resolution structural framework derived from the integration of primary magnetic data, satellite gravity inversion, and geological observations, the results are expected to contribute to geothermal exploration strategies, particularly in improving the understanding of structural controls on non-volcanic geothermal systems and supporting future renewable energy development in tectonically active regions of Indonesia.

2. METHODS

This study adopts a multi-method approach to investigate subsurface characteristics in the geothermal prospect area of Karangrejo, Pacitan. Ground magnetic measurements provide information on the distribution of magnetic minerals and subsurface geological structures. These data were collected on a grid with station spacing of 400–500 m, adjusted based on field obstacles, covering a total area of 25 km². Complementing the magnetic method, GGMPlus satellite gravity data with higher spatial resolution (approximately 220-meter point spacing) is utilized to estimate subsurface rock density variations, which may indicate the presence of intrusive rock bodies or significant geological structures, including possible estimation of fracture porosity [21]. These two geophysical datasets covering an area of 25 km², are integrated with surface geological data to provide a more comprehensive understanding of the geothermal system in the study area.

2.1. Magnetic Method Approach

Magnetic data that has undergone daily variation correction, IGRF correction, and reduction to the pole (RTP) is subsequently subjected to regional and residual anomaly separation. This step distinguishes the effects of deeper regional magnetic fields from shallower local anomalies. Consequently, applying Tilt Derivative (TDR) analysis to the residual anomalies becomes more effective in identifying the boundaries of geological structures targeted in the study, such as faults, folds, or intrusive bodies, thereby enhancing the accuracy and detail of data interpretation. Principally, residual anomalies are utilized to identify zones of low magnetic intensity, which serve as indicators for geothermal reservoirs [22]. This value is associated with heat or thermal change that diminish the magnetic intensity [23-24]. Preliminary analysis employs the Tilt Derivative (TDR) technique to map geological structures, such as faults and fractures, which are critical for hot fluid migration [25].

The Tilt Derivative Filter is an effective magnetic data processing technique for identifying and mapping subsurface geological structures. This method works by calculating the vertical and horizontal derivatives of the magnetic field anomaly, producing a map that emphasizes anomaly continuity, which indicates lithological boundaries or geological structures. Tilt derivative values range from $-\pi/2$ to $+\pi/2$, with the zero-crossing of the tilt derivative indicating the edges of the anomaly source. This feature aids in estimating the orientation of geological structures [26-27]. The TDR Filter is mathematically shown by Eq. (1):

DOI: https://doi.org/10.17509/ijost.v11i1.93666
p- ISSN 2528-1410 e- ISSN 2527-8045

$$\mathrm{TDR} = \frac{\frac{\partial T}{\partial z}}{\sqrt{\left(\frac{\partial T}{\partial \mathrm{x}}\right)^2 + \left(\frac{\partial T}{\partial \mathrm{y}}\right)^2}} \tag{1}$$

2.2 Satellite Gravity (GGMPlus) Method Approach

The GGMPlus satellite gravity data for the study area was obtained from https://ddfe.curtin.edu.au/gravitymodels/GGMplus/data/ga/. This model integrates GRACE, GOCE, EGM2008 data, and topography from SRTM and SRTM30_PLUS to represent gravity variations from regional to local scales. The application of Residual Terrain Modeling (RTM) allows the estimation of high-frequency gravity signals (~10 km to ~250 m), which are crucial for the identification of local-scale mass anomalies. Based on a comparison between terrestrial gravity data and gravity model results (Satellite-only, GGE, and GGMPlus) conducted by Hirt *et al.,* [28], it is known that the GGMPlus model shows the best accuracy with the smallest RMS value in the three test areas (United States, Australia, and Switzerland), which is in the range of 2.9–4.4 mGal, making it the most reliable model to be used as supporting data.

This raw data underwent a processing sequence that included several corrections: latitude correction, free-air correction, density estimation, Bouguer correction, and terrain correction. These corrections eliminate non-geological influences, such as the Earth's shape, elevation, and density variations in the overlying rock layers, so that the remaining gravity anomalies can be interpreted as variations in subsurface rock density. The resulting complete Bouguer anomaly map was further separated into regional and residual components to distinguish the effects of large-scale and small-scale geological structures using an upward continuation filter [29].

For magnetic data that has been reduced to the pole (RTP), we use the ZondGM3D software to perform 3D inversion modeling. In solving inversion problems, various methods of deconvolution and Newton's method with focused regularization are applied. The process is described by Eq. (2):

$$(A^T W^T WA + \mu C^T RC)\Delta m = A^T W^T \Delta f - \mu C^T RCm \tag{2}$$

where A, also known as the Jacobian matrix, contains the partial derivatives of the measured data concerning the model parameters. The operator C is used to produce a smoother model. The matrix W provides information about the confidence level of each measured data point. The vector m represents the model parameters to be determined. The regularization parameter μ balances the trade-off between the model's fit to the data and the model's smoothness. The residual vector Δf indicates the difference between the values predicted by the model and the actual measured values. Finally, the focus operator R emphasizes specific characteristics within the model.

Inversion modeling aims to determine model parameters that produce responses that match the observed data. For this reason, inversion modeling is often called data fitting modeling. The Complete Bouguer Anomaly (gravity) data was inverted using Grablox 1.6 software developed by several researcher. The resulting 3D model can be visualized in either 2D or 3D formats [30]. The Grablox software combines two inversion methods: Singular Value Decomposition (SVD) Inversion and Occam Inversion, which are processed [31].

The Singular Value Decomposition technique decomposes a matrix into simpler components, akin to factoring a number. According to Zhao and Ye [32], a matrix A can be

DOI: https://doi.org/10.17509/ijost.v11i1.93666
p- ISSN 2528-1410 e- ISSN 2527-8045

decomposed into two new matrices, *U* and *V*. Mathematically, the relationship between these matrices can be expressed in Eq. (3), as presented by Sugianto and Rahadinata [33].

$$A = U\,S\,V^T \tag{3}$$

In the equation, *U* and *V* are special matrices referred to as the left and right orthogonal matrices, respectively, while *S* is a diagonal matrix. The advantage of the SVD technique lies in its ability to stabilize matrix inversion calculations. The Occam Inversion method, on the other hand, addresses non-linear problems by employing a linear approach. This inversion method utilizes the roughness level of a model [34]. The Occam equation is presented in Eq. (4):

$$U = \left|\left|\eth m\right|\right|^2 + \mu^{-1}\left\{\left|\left|Wd - WGm\right|\right|^2 - X^2\right\} \tag{4}$$

where $\left|\left|\eth m\right|\right|^2$ represents the roughness, a μ^{-1} is the Lagrange multiplier, $\left|\left|Wd - WGm\right|\right|^2$ is the misfit, and X^2 denotes the error.

In developing inversion problem solutions, special attention is given to creating the initial model, such as individual measurement weights and the possible range of parameters, as these factors significantly influence the final results of the inversion modeling. The two inversion models obtained will be integrated to analyze the geothermal system in the Karangrejo-Tinatar area.

3. RESULTS AND DISCUSSION

Based on the processed magnetic and satellite gravity data, the RTP (Reduce to Pole) map and CBA (Complete Bouguer Anomaly) map are presented in **Figures 1b** and **1c**, respectively. The magnetic data results indicate a range of values from -281 to 173 nT, while the gravity data results show gravitational anomalies ranging from 164.6 to 169.1 mGal. A geological map from prior field mapping is provided in **Figure 1a** to facilitate interpretation. Igneous and volcanic rocks dominate the study area, such as andesite, breccia, and tuff. Six geophysical-geological zones were identified within the study area (summarised in **Table 1**). Zones 1 and 6, located in the northwest and northeast respectively, are associated with moderate-to-high magnetic and gravity anomalies, consistent with breccia and andesite lava. Zone 2, near the Tinatar geothermal manifestations, displays high anomalies in both datasets and is characterised by andesite lava with galena-bearing rocks exhibiting elevated magnetisation. Zones 3 and 5, in the southwest and east, show low-to-moderate anomalies reflecting tuff and breccia lithologies of relatively low density. Zone 4 in the southeast is dominated by poorly compacted tuff and alluvial deposits, producing the lowest anomaly values across both datasets.

To analyze the structures controlling geothermal manifestations in the Karangrejo and Tinatar areas, Tilt Derivative (TDR) analysis was conducted on magnetic data based on the RTP map results. Additionally, this data was correlated with the distribution of residual anomaly values derived from satellite gravity methods. The interpretation of suspected fault structures was further supported by geological maps (**Figure 1a**). Indications of fault structures or anomaly edges on the magnetic TDR map (**Figure 2a**) are represented by regions with zero contour values or areas between high and low anomalies (white-colored regions). Meanwhile, structural analysis on the residual anomaly map (**Figure 2b**) using the gravity method is marked by moderate anomalies (yellow-colored regions).

DOI: https://doi.org/10.17509/ijost.v11i1.93666
p- ISSN 2528-1410 e- ISSN 2527-8045

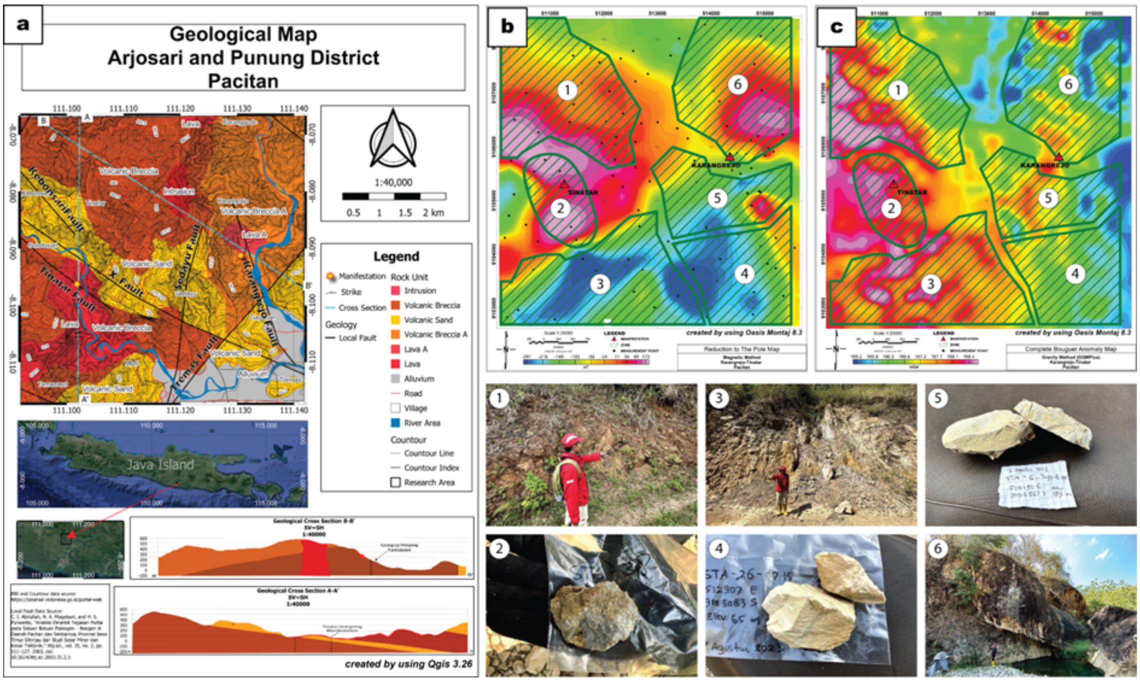

Figure 1. Result Map; (a) Local geological map; (b) Magnetic anomaly map (Reduced to the poles); (c) Complete Bouguer Anomaly map in Karangrejo and Tinatar, Pacitan Regency

Table 1. Integration of magnetic and gravity anomaly maps with geological mapping data

Zone	Magnetic	Gravity	Type of Rock
1	Moderate to High	Moderate to High	Breccia
2	High	High	Lava Andesite & Breccia
3	Low to Moderate	Moderate to High	Breccia & Tuff
4	Low	Low	Tuff & Alluvium
5	Low to Moderate	Low to Moderate	Tuff
6	High	Moderate	Breccia & Lava Andesite

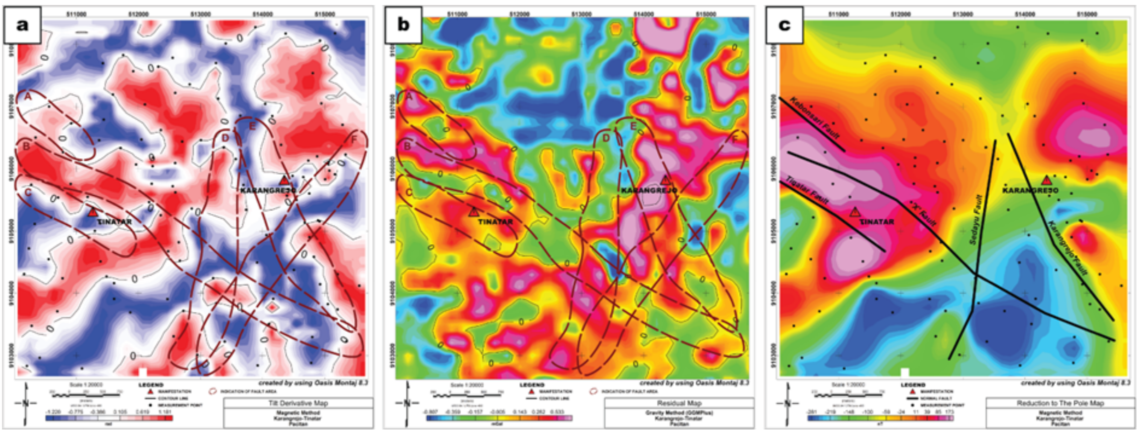

Figure 2. (a) Geological structure analysis using magnetic TDR maps; (b) Residual gravity maps; (c) Magnetic RTP map.

Five out of six structures from the geological map were well-identified using magnetic TDR analysis and residual gravity anomalies. Area A, oriented northwest-southeast, spans 1.5 km in length, and the fault in this area is identified in both the TDR map and residual anomalies. This fault is named the Kebonsari Fault. Area B, also oriented northwest-southeast, spans 6.5 km, and its fault is identified in both the TDR map and residual anomalies. However, its

DOI: https://doi.org/10.17509/ijost.v11i1.93666
p- ISSN 2528-1410 e- ISSN 2527-8045

position shifts slightly compared to the geological map due to adjustments from derivative analysis, and it is named 'Fault X'. Area C, oriented northwest-southeast with a length of 2 km, also shows an identified fault in both the TDR map and residual anomalies. This fault is named the Tinatar Fault and is presumed to control geothermal manifestations, particularly the Tinatar hot springs. Area D, oriented north-south, spans 4 km and shows a reasonably clear fault identified in the TDR map and residual anomalies, named the Sedayu Fault. Area E, oriented northwest-southeast with a length of 3.5 km, also displays an identified fault in the TDR map and residual anomalies, named the Karangrejo Fault. This fault is suspected to control the emergence of the Karangrejo hot springs. Area F, oriented northeast-southwest with a length of 4.5 km, is moderately identified in the residual anomaly map but is less distinct in the TDR map. Due to its unclear identification, this fault is excluded from subsequent analysis stages. These findings align with studies by [18, 35-36]. Which states that there are Karangrejo and Tinatar faults which control the emergence of geothermal manifestations. All identified faults are subsequently overlaid on the RTP map, as shown in **Figure 2c**, with a summarized description provided in **Table 2**.

Table 2. Geological fault structure analysis.

Fault name (Geological Map)	Area	Magnetic	Gravity (GGMPlus)	Identified or Not Identified
		TDR	Residual	
Kebonsari Fault	A	✓	✓	Identified
X Fault	B	✓	✓	Identified
Tinatar Fault	C	✓	✓	Identified
Sedayu Fault	D	✓	✓	Identified
Karangrejo Fault	E	✓	✓	Identified
Tremas Fault	F		✓	Not Identified

To gain a more comprehensive understanding of the subsurface structures controlling the geothermal system, a 3D inversion analysis based on gravity and magnetic anomaly data is necessary. The 3D inversion approach is employed because both total gravity anomalies and magnetic anomalies result from variations in density distribution based on the difference between observed gravity data and theoretical gravity values and variations in magnetic susceptibility based on the difference between observed and predicted magnetic anomalies. Several important factors must be considered when constructing constraints or an initial model to ensure optimal inversion accuracy in both gravity and magnetic inversion processes. Key factors to consider in constructing constraints or initial models include cell size, inversion depth, and the threshold for absolute error [37].

ZondGM3D is software for three-dimensional gravity and magnetic data interpretation, applicable to land and airborne surveys. Magnetic surveys examine the field generated by rocks containing ferromagnetic minerals. The relationship between the measured field on the surface and the magnetic properties of the rocks allows for the inference of magnetic objects' presence. ZondGM3D uses a simple and clear data format, enabling the combination of various observation systems, including various topographic settings and additional information. The modeling process provides an opportunity to select optimal parameters for the observation system to solve the formulated geological problems.

3D magnetic inversion modeling using ZondGM3D software has been applied to the Karangrejo-Tinatar geothermal area to reveal detailed subsurface geological structures and geothermal fluid flow pathways shown in **Figure 3**. This analysis utilizes magnetic data with a cell resolution of 5 × 5 km in the horizontal plane and 2 km in depth, which has undergone pole reduction. The lowest susceptibility is determined to be $10 \times 10^{-4}\ \chi m$, while the highest susceptibility is $30 \times 10^{-4}\ \chi m$. To convert the χ values in the CGS system used in the program, the magnetic susceptibility in SI units is divided by 4π.

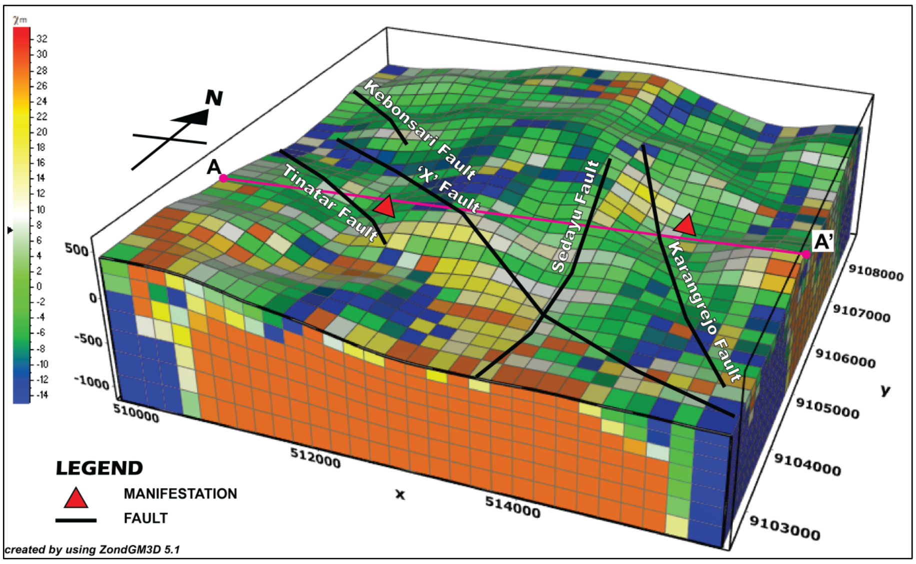

Figure 3. 3D model of rock susceptibility in Karangrejo and Tinatar, Pacitan Regency.

The inversion results show significant variations in magnetic susceptibility, as shown in **Figure 3**, ranging from -0.01759 to 0.0402 SI, indicating differences in the magnetic properties of the subsurface rocks. There are significant areas where the magnetic susceptibility values are equal to or less than zero (**Figure 4**), indicating the absence of magnetic susceptibility in those regions. Magnetic susceptibility values equal to or less than zero are significant because they indicate no magnetic response in those areas. The absence of magnetic susceptibility can be associated with diamagnetic properties, referring to materials with negative magnetic susceptibility that do not enhance external magnetic fields. This phenomenon may also be caused by high temperatures leading to the loss of magnetization. High temperatures can erase the magnetic properties of materials, making them unresponsive to magnetic fields. In other words, high temperatures have removed the magnetization of the material, leaving behind diamagnetic characteristics as one of the possible causes [37-38].

The initial stage of the 3D gravity inversion process is creating the initial model. This initial model will be processed using Singular Value Decomposition (SVD) and Occam inversion with Grablox software. The data input for creating this 3D model is the Complete Bouguer Anomaly data. Parameters for the initial model include a main block with dimensions of 20 x 20 x 10, from which 4000 minor blocks with dimensions of 5 x 5 x 1.4 km (length x width x height) are obtained. Furthermore, the determination of the initial model's lowest density value of 1.9 g/cm³ is based on the lowest density rock type in the study area, which is tuff with a density range of 1.9 - 2.5 g/cm³. Meanwhile, the highest-density rock type in the study area is andesite lava, with a density range of 2.4 - 3.1 g/cm³. The density parameter is determined using the Parasnis method, resulting in a value of 2.671 g/cm³.

Figure 5 presents the results of satellite gravity inversion modeling, indicating a range of rock density variations in the study area from 1.88 to 3.11 g/cm³. The model shows a dominance of low to moderate-density rocks (1.88-2.88 g/cm³) at the top, interpreted as pyroclastic rocks such as tuff and breccia at the surface. In contrast, the deeper parts of the model are dominated by high-density rocks (2.88-3.11 g/cm³), indicating the presence of andesitic rocks. A low-density anomaly (1.88-2.17 g/cm³) is identified in the southeastern

DOI: https://doi.org/10.17509/ijost.v11i1.93666
p- ISSN 2528-1410 e- ISSN 2527-8045

part, likely representing alluvial deposits accumulated in low-lying topographic areas due to sedimentation.

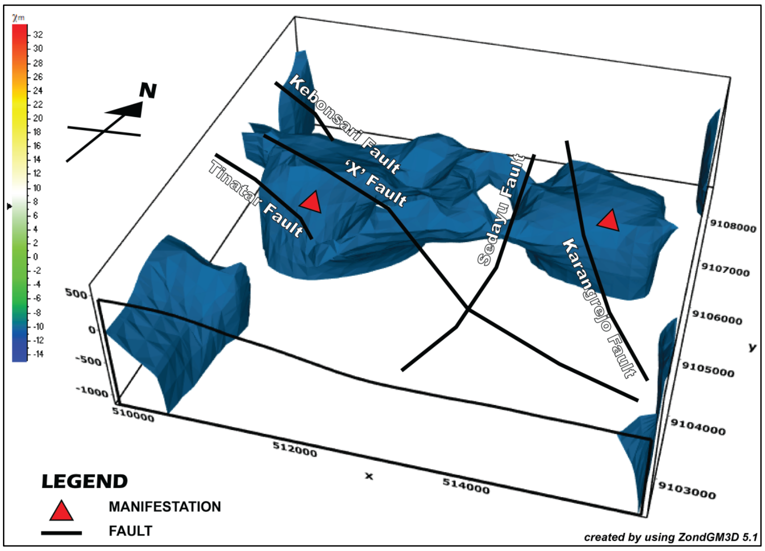

Figure 4. 3D model of low rock susceptibility in Karangrejo and Tinatar, Pacitan Regency.

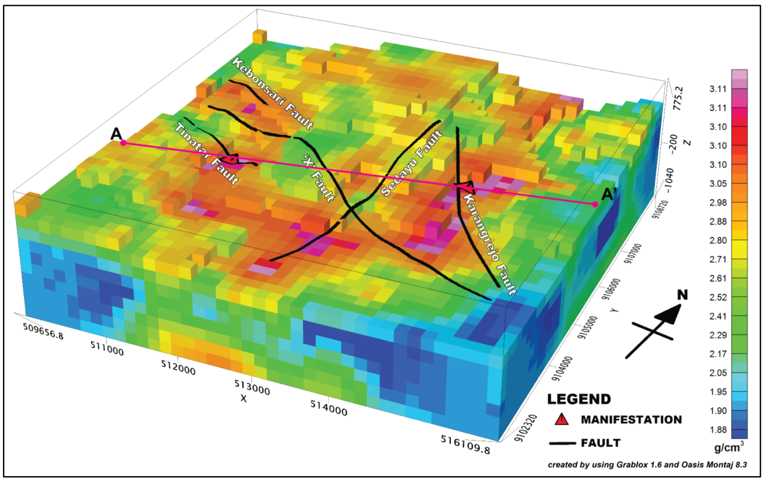

Figure 5. 3D model of rock density in Karangrejo and Tinatar, Pacitan Regency.

To further understand the geothermal potential in the study area, we analyzed the correlation between the density model and the magnetic susceptibility of the rocks from the 3D inversion results. The results revealed an interesting pattern: areas with higher rock densities (2.9-3.1 g/cm³) (**Figure 6**) tend to have lower magnetic susceptibility values (-0.01759 to -0.08 SI) (**Figure 4**). This pattern extends from the geothermal manifestations in Tinatar to Karangrejo, indicating a correlation between high density, high temperature, and geothermal potential. These findings support the hypothesis that heat transfer from the Karangrejo-Tinatar geothermal system contributes to the temperature increase in these areas, as reflected by the high-density values and low magnetic susceptibility [37].

The comparative analysis between the density profile and magnetic susceptibility profile in **Figures 7a** and **7b**, which cross the geothermal manifestation zones of Karangrejo and Tinatar along the A-A' transect, provides a clearer picture of the correlation between geological structures and the distribution of geothermal fluids. The continuity of fault structures previously identified through TDR analysis, such as the Karangrejo, Tinatar, X, and

DOI: https://doi.org/10.17509/ijost.v11i1.93666
p- ISSN 2528-1410 e- ISSN 2527-8045

Sedayu faults, is observable in both profiles. This suggests that these faults play a crucial role in controlling the flow of geothermal fluids.

Additionally, the magnetic susceptibility profile indicates the presence of a hydrothermal alteration zone around the faults, characterized by relatively lower susceptibility values due to changes in rock mineralogy. Meanwhile, the density profile shows significant density contrasts around the faults, likely caused by differences in lithology or the porosity of the rocks. Based on this analysis, it can be concluded that the Karangrejo and Tinatar faults act as the main discharge zones for geothermal fluid manifestations. In contrast, the X and Sedayu faults serve as recharge zones that facilitate the infiltration of meteoric water into the geothermal system.

Figure 7c presents a comprehensive visualization of the relationship between geological structures, rock physical properties, and geothermal fluid flow in the study area. This integrated view combines the magnetic susceptibility model **(Figure 7a)** and density model (**Figure 7b**) with geological structure analysis. The simulated heat migration pathways indicate that the primary heat source is located beneath the Tinatar manifestation, consistent with earlier findings by several researcher. Heat from this source moves vertically through fracture and fault zones before reaching the surface in the Karangrejo and Tinatar areas. Zones exhibiting low magnetic susceptibility and high density in **Figure 7c** suggest the presence of alteration minerals resulting from geothermal fluid interaction with host rocks, further supporting the interpretation that the depicted heat migration paths represent dominant fluid flow pathways.

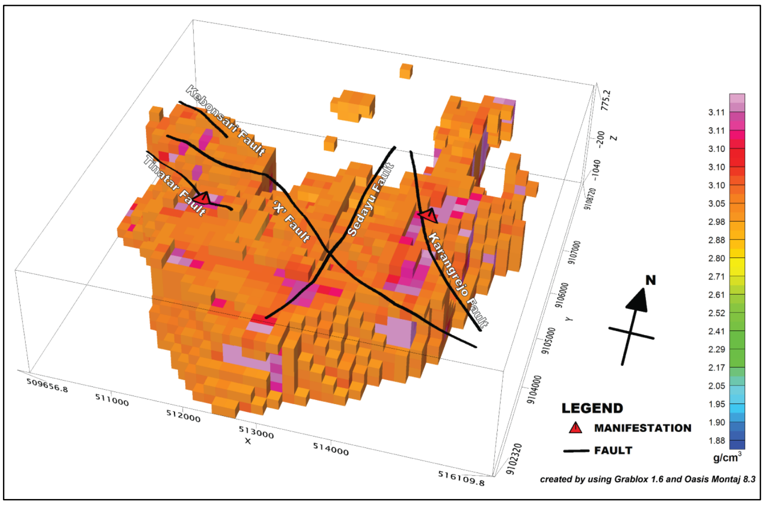

Figure 6. 3D model of high rock density in Karangrejo and Tinatar, Pacitan Regency.

The structural framework identified in this study carries significant implications for geothermal exploration strategies in Indonesia, particularly for tectonically controlled, low-temperature prospects. Delineation of major fault zones as recharge and discharge pathways provides practical guidance for prioritizing drilling locations and improving early-stage exploration efficiency. The integration of primary magnetic data, satellite-derived gravity modeling, and geological analysis demonstrates an effective approach for reducing subsurface uncertainty in complex geothermal settings. Such methodologies are especially relevant for developing underexplored non-volcanic resources, thereby contributing to Indonesia's renewable energy transition targets.

Despite the effectiveness of gravity and magnetic methods in delineating shallow subsurface structures and alteration zones, these potential field techniques have inherent limitations in directly resolving deeper geothermal heat sources. The inversion models

DOI: https://doi.org/10.17509/ijost.v11i1.93666
p- ISSN 2528-1410 e- ISSN 2527-8045

presented in this study are constrained to depths of approximately less than 2000 m, reducing sensitivity to deeper bodies with low physical property contrasts. Future exploration stages would benefit from the integration of deeper-penetrating geophysical techniques such as magnetotelluric surveys and passive or tomographic seismic investigations to better constrain reservoir geometry, fracture networks, and heat source distribution. Complementary geochemical analyses, including geothermometry and isotope studies, are also recommended to improve reservoir temperature estimation and fluid origin interpretation. Furthermore, incorporating environmental impact considerations and community-based risk mitigation strategies will be essential for supporting sustainable geothermal exploration and enhancing public acceptance of geothermal energy development in structurally controlled non-volcanic regions.

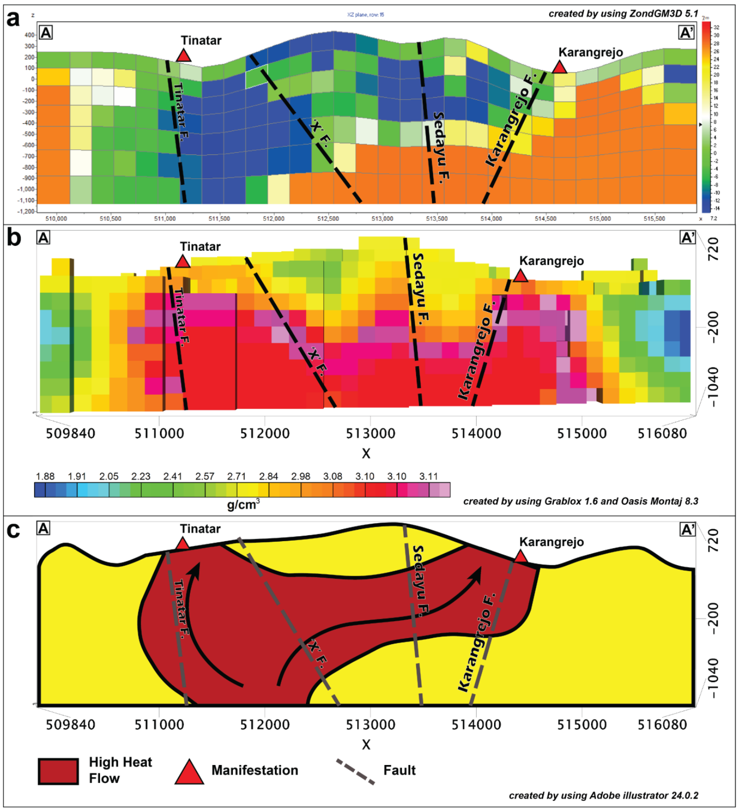

Figure 7. (a) The cross-section A-A' Karangrejo-Tinatar shows the distributions of densities; (b) The distribution of susceptibilities; (c) The simulated image of the migration path of heat flows originating from the source to the identified geothermal potential area.

4. CONCLUSION

This study demonstrates that the integration of primary ground magnetic measurements, satellite-derived gravity data, and geological observations provides an effective approach for characterizing structurally controlled geothermal systems in non-volcanic settings. The inversion results reveal significant variations in magnetic susceptibility (−0.01759 to 0.0402 SI) and rock density (1.88 to 3.11 g/cm³), indicating strong contrasts in subsurface physical properties associated with geothermal processes. The comparative analysis of susceptibility and density models highlights a spatial correlation between low magnetic susceptibility and high-density zones, interpreted as areas affected by thermal alteration and heat transfer toward surface geothermal manifestations. Structural interpretation successfully identified five major faults—Kebonsari, X, Karangrejo, Sedayu, and Tinatar—that function as key

DOI: https://doi.org/10.17509/ijost.v11i1.93666
p- ISSN 2528-1410 e- ISSN 2527-8045

pathways controlling geothermal fluid circulation, acting respectively as recharge and discharge zones within the system. For the first time, the integration of primary ground magnetic surveys with satellite gravity data has produced a coherent 3D structural model of the Karangrejo–Tinatar geothermal prospect, identifying five controlling fault structures and delineating their roles as either recharge (X, Sedayu) or discharge (Karangrejo, Tinatar) zones within the hydrothermal system.

5. ACKNOWLEDGMENT

The author's thanks go to the team from Brawijaya Volcano and Geothermal Research Center (BRAVO GRC) of Brawijaya University, Malang, Indonesia, who have provided full assistance and support during the field acquisition process, data processing, and model interpretation. This research was funded by Directorate of Research and Community Services, Brawijaya University on a Grant for enhancing the research ecosystem for professors under contract number 00144.12/UN10.A0501/B/PT.01.03.2/2024. Furthermore, the publication of this research was partially supported by Brawijaya University through the Adjunct Professor Program (Batch 3) for Fiscal Year 2025 under contract number 06408/UN10.F0901/B/TU/2025.

6. AUTHORS' NOTE

The authors declare that there is no conflict of interest regarding the publication of this article. The authors confirmed that the paper was free of plagiarism.

7. REFERENCES

[1] Ouerghi, F. H., Omri, M., Nisar, K. S., El-Aziz, R. M. A., and Taloba, A. I. (2024). Investigating the potential of geothermal energy as a sustainable replacement for fossil fuels in commercial buildings. *Alexandria Engineering Journal, 97*, 215–229.

[2] Bloomfield, K. K., Moore, J., and Neilson, R. N. (2003). Geothermal energy reduces greenhouse gases. *Geothermal Resources Council Bulletin, 32*(2), 77–79.

[3] Ariyanto, S. V., and Susilo, A. (2014). Estimation of magma chamber structure of Kelud Volcano based on gravity data using equivalent point mass method. *Natural B, 2*(3), 229–234.

[4] Jaya, L. O. M. G., Suprayogi, A., Sudarsono, and Hasbi, M. (2021). Identification of non-volcanic geothermal manifestation in North Konawe Regency, Indonesia, using land surface temperature of Landsat satellite image. *IOP Conference Series: Earth and Environmental Science, 622*, 012040.

[5] Arrasyid, H., Maryanto, S., Wuryani, S. D., Santoso, D. R., and Subagiyo, A. (2024). Integration of microtremor and PS-InSAR analysis to investigate the susceptible area in the Pronojiwo District (Indonesia) following the 2021 East Java M6.1 earthquake. *Annals of Geophysics, 67*(2), SE216.

[6] Khodayar, M., and Björnsson, S. (2024). Conventional geothermal systems and unconventional geothermal developments: An overview. *Open Journal of Geology, 14*(2), 196–246.

[7] Ivana, J., Larasati, T., Chandra, V. R., Wibowo, A. E. A., Darmawan, D., Fadhillah, F. R., Permadi, G. B., Shalihin, M. G. J., Mustika, A. I., and Baxter, C. (2024). 3D model of Bora Pulu non-volcanic geothermal prospect, Central Sulawesi, Indonesia. In *Proceedings of the 49th Workshop on Geothermal Reservoir Engineering* (SGP-TR-227, pp. 1–14).

[8] Purnomo, B. J., and Pichler, T. (2014). Geothermal systems on the island of Java, Indonesia. *Journal of Volcanology and Geothermal Research, 285*, 47–59.

[9] Zayed, M. E., Shboul, B., Yin, H., Zhao, J., and Zayed, A. A. A. (2023). Recent advances in geothermal energy reservoirs modeling: Challenges and potential of thermo-fluid integrated models for reservoir heat extraction and geothermal energy piles design. *Journal of Energy Storage, 62*, 106835.

[10] Boling, R. A., Tanesib, J. L., Sutaji, H. I., Lapono, L. A. S., and Lewerissa, R. (2024). Re-evaluation of a geothermal system model based on high-resolution gravity field inversion: A case study of the Maritaing geothermal field, Alor Regency, East Nusa Tenggara Province, Indonesia. *Kuwait Journal of Science, 51*(2), 100187.

[11] Spijkerboer, R. C., Turhan, E., Roos, A., Billi, M., Vargas-Payera, S., Opazo, J., and Armiero, M. (2022). Out of steam? A social science and humanities research agenda for geothermal energy. *Energy Research and Social Science, 92*, 102801.

[12] Adhitia, I., and Karmadi, M. A. (2021). Geothermal potential study in Bogor Regency based on geology and geochemistry. *Journal of Engineering, 22*(1), 27–37.

[13] Mulyani, S., Daud, Y., Pasiki, R. G., and Siagian, H. (2022). Fault structure characterization in geothermal field X (Sumatra) based on geological mapping, remote sensing, and gravity data. *Bulletin of Geological Resource, 17*(2), 109–124.

[14] Afni, G. N., and Kusmita, T. (2021). Identification of the tectonic structure of the non-volcanic geothermal system in the Nyelanding and Permis areas of South Bangka using the gravity method. *Jurnal Riset Fisika Indonesia, 2*(1), 1–6.

[15] Firdaus, R., Oktaviyani, S., Hardianti, P., Kusmita, T., and Indriawati, A. (2021). Identification of subsurface rock structure of non-volcanic geothermal systems based on gravity anomalies (Terak Village, Central Bangka Regency). *Journal of Applied Geospatial Information, 5*(2), 542–547.

[16] Safani, J., Wirawan, R., Ibrahim, K., Masri, and Mokui, H. T. (2026). Investigation of geothermal system using advanced processing and inversion of gravity data in Lainea non-volcanic geothermal field, Indonesia. *Rudarsko-Geološko-Naftni Zbornik, 41*(1), 143–156.

[17] Wei, C., Guan, Y., Li, X., Sun, M., and Wu, Y. (2025). Exploration of shallow geothermal resources based on gravity and magnetic 3D inversion in the Wudalianchi–Laoheishan Volcano and surrounding areas. *Energies, 18*(8), 2011.

[18] Puspita, M. B., Aprilla, A. N., Maryanto, S., and Sari, R. P. H. (2024). Preliminary study of subsurface geological setting based on gravity anomalies in Karangrejo-Tinatar geothermal area, Pacitan Regency, Indonesia. *International Journal of Geophysics, 2024*(1), 9976867.

[19] Widiyansari, R., Fatimah, S., Risti, F., Hikmah, N., Darmawan, D., Aziz, K. N., and Fitrianingtyas, R. (2025). Analysis of the subsurface structure of the Pacitan geothermal area based on GGMPlus gravity data. *Progressive Physics Journal, 6*(2), 594–607.

[20] Sumotarto, U., Hendrasto, F., Meirawati, M., and Azzam, I. (2020). Geology of Arjosari geothermal area, Pacitan, East Java. *AIP Conference Proceedings, 2245*(1), 070001.

[21] Altwegg, P., Schill, E., Abdelfettah, Y., Radogna, P. V., and Mauri, G. (2015). Toward fracture porosity assessment by gravity forward modeling for geothermal exploration (Sankt Gallen, Switzerland). *Geothermics, 57*, 26–38.

[22] Lestari, F. A., Maryanto, S., and Santoso, D. R. (2019). Continuity reservoir magnetic anomaly at Kelud, Kasinan-Songgoriti, and Arjuno-Welirang of geothermal area, East Java, Indonesia. *SSRG International Journal of Applied Physics, 6*(3), 111–117.

DOI: https://doi.org/10.17509/ijost.v11i1.93666
p- ISSN 2528-1410 e- ISSN 2527-8045

[23] Salem, A., Ravat, D., Smith, R., and Ushijima, K. (2005). Interpretation of magnetic data using an enhanced local wavenumber (ELW) method. *Geophysics, 70*(2), L7–L12.

[24] Alqahtani, F., Ehsan, M., Aboud, E., Abdulfarraj, M., and El-Masry, N. (2023). Integrated approach using petrophysical, gravity, and magnetic data to evaluate the geothermal resources at the Rahat Volcanic Field, Saudi Arabia. *Frontiers in Earth Science, 11*, 11356.

[25] Kasidi, and Suryanto, W. (2022). Application of tilt derivative (TDR) for fault structure identification in Bur Ni Geureudong geothermal field, Aceh, Indonesia. *International Journal of Geophysics, 2022*(1), 1–12.

[26] Miller, H. G., and Singh, V. (1995). Potential field tilt—A new concept for location of potential field sources. *Journal of Applied Geophysics, 32*(2), 213–217.

[27] Asma, Hamimu, L., Rubaiyn, A., and Asfar, S. (2020). Fault zone identification based on magnetic anomaly data analysis in Lainea area, South Konawe Regency, Southeast Sulawesi. *Indonesian Journal of Geophysical Engineering, 2*(3), 47–57.

[28] Hirt, C., Claessens, S., Fecher, T., Kuhn, M., Pail, R., and Rexer, M. (2013). New ultra-high resolution picture of Earth's gravity field. *Geophysical Research Letters, 40*(16), 4279–4283.

[29] Kebede, H., Alemu, A., and Fisseha, S. (2020). Upward continuation and polynomial trend analysis as a gravity data decomposition, case study at Ziway-Shala Basin, Central Main Ethiopian Rift. *Heliyon, 6*(1), e03292.

[30] Hightower, E., Gurnis, M., and Van Avendonk, H. (2020). A Bayesian 3-D linear gravity inversion for complex density distributions: Application to the Puysegur subduction system. *Geophysical Journal International, 223*(3), 1899–1918.

[31] Maimuna, A. K., Pramesthi, E. A., Segoro, Y. A., Margiono, R., Azzahra, K. S., Akhadi, M., and Siregar, D. V. (2021). Gravity anomaly analysis using SVD method and 3D modeling (Case study of earthquakes in Togean Islands, Tojo Una-Una Regency, Sulawesi). *Journal of Geophysics, 19*(1), 17–23.

[32] Zhao, X., and Ye, B. (2016). Singular value decomposition packet and its application to extraction of weak fault feature. *Mechanical Systems and Signal Processing, 70–71*, 73–86.

[33] Sugianto, A., and Rahadinata, T. (2015). 3D gravity modeling of the Dolok Marawa geothermal area, Simalungun Regency, North Sumatra. *Bulletin of Geological Resource, 10*(2), 26–39.

[34] Constable, S. C., Parker, R. L., and Constable, C. G. (1987). Occam's inversion: A practical algorithm for generating smooth models from electromagnetic sounding data. *Geophysics, 52*(3), 289–300.

[35] Abdullah, C. I., and Purwanto, N. A. M. H. S. (2003). Dynamic analysis of paleostress in Paleogene–Neogene rock units in the Pacitan area and surroundings, East Java Province, based on minor fault and tectonic fracture studies. *Proceedings of ITB Science and Technology, 35*(2), 111–127.

[36] Puspita, M. B., Perwita, C. A., Maryanto, S., and Suyanto, I. (2023). Magnetic method analysis in geothermal manifestation area of Karangrejo, Pacitan Regency. *INSOLOGI: Journal of Science and Technology, 2*(5), 907–916.

[37] Gaber, G. M., Saleh, S., and Kotb, A. (2024). 3D gravity and magnetic inversion modelling for geothermal assessment and temperature modelling in the central eastern desert and Red Sea, Egypt. *Scientific Reports, 14*(1), 1–16.

[38] Li, Z., and Fu, G. (2019). Application of magnetic susceptibility parameters in research of igneous rock in Chepaizi. *Journal of Physics: Conference Series, 1176*(4), 042068.

DOI: https://doi.org/10.17509/ijost.v11i1.93666
p- ISSN 2528-1410 e- ISSN 2527-8045